Feras S. Alhejji, et. al. International Journal of EngineeringResearch and Applications
www.ijera.com
ISSN: 2248-9622, Vol. 13, Issue 12, December 2023, pp115-137

RESEARCH ARTICLE OPEN ACCESS

Techno-Economic Analysis of PV Water Pumping Systems for Agriculture Purposes in the Kingdom of Saudi Arabia

Feras S. Alhejji, A. F. Almarshoud

Feras S. Alhejji
O&MDepartment, Military construction, Ministry of Defence, Saudi Arabia
f-966966@hotmail.com

A. F. Almarshoud
Department of EE, College of Engineering, Qassim University, Saudi Arabia
e-mail: dr_almarshoud@qec.edu.sa, dr_almarshoud@qu.edu.sa
ORCID: 00000001-9818-7827

ABSTRACT
This study conducts a thorough examination of the technical and economic aspects of solar water pumping systems for agricultural use in six distinct regions of Saudi Arabia: Qassim, Al Ahsa, Al Kharj, Al Jouf, Hail, and Wadi Aldoaser. The technical assessment delves into crucial factors, including solar radiation levels, local climate conditions, pump system types, groundwater levels, and daily water demand. It identifies certain energy output limitations and proposes three potential solutions. The economic feasibility has been evaluated using the life cycle costing method, considering local market prices. The economic analysis relies on key financial indicators, including the Levelized Cost of Produced Water, the Levelized Cost of generated Energy, and the Payback Period. We explore these analyses in the context of three suggested solutions, encompassing both standalone and grid-connected modes of operation. Among these solutions, the second option, involving tilt angle control, emerges as the most economically favorable choice. It exhibits the lowest average values for both the Levelized Cost of Water and the Levelized Cost of Energy. Additionally, this option features the shortest payback period across all analyzed wells, regardless of the operational mode. Based on the comprehensive nature of our analyses, we highly recommend the second option as the preferred solution for solar water pumping applications in Saudi Arabian agriculture.

Keywords: Sustainable irrigation; PV water pumping; solar energy water pumping; Solar irrigation; solar energy economics.

Date of Submission: 12-12-2023 Date of acceptance: 26-12-2023

I. Introduction

The agricultural sector in Saudi Arabia heavily relies on underground water sources, necessitating significant amounts of electricity or diesel fuel to extract water from deep wells. With the recent implementation of increased electricity tariffs in Saudi Arabia and the remarkable reduction in the cost of solar panels, harnessing solar energy as an alternative energy source for water pumping and irrigation holds great promise. This article explores various aspects of this transition.

Researchers have directed their focus toward assessing the economic feasibility of photovoltaic (PV) water pumping systems, taking into account location-specific factors and climate conditions in rural or remote regions [1-2]. They have explored the performance of PV-powered water pumping systems under varying climatic conditions and static head variations [3-5]. Control strategies aimed at optimizing PV system performance and comprehensive economic assessments have also been elaborated [6-7].

Additionally, researchers have conducted comparative studies to determine the optimal performance criteria for standalone photovoltaic water pumping systems using both direct current and alternating current motors [8]. Belkacem Bouzidi explored two scenarios, considering factors like loss of probability and storage factor, to ascertain optimal configurations [9]. Furthermore, researchers have investigated multiple objective

functions, including loss of load probability, life cycle cost, and excess water volume, to optimize algorithm-based sizing of standalone photovoltaic water pumping systems [10].

Efforts by Zaheb et al. [11] resulted in an effective PV water pumping system, accompanied by theoretical and modeling studies of all system components. Their work also involved a comparative analysis using two optimization techniques: perturb and observe (P&O) and fuzzy maximum power point algorithms. A collaborative project by A. Gundodgdu and B. Gure led to the design and implementation of a low-cost, standalone 2.2 kW PV pumping system, with a detailed examination of design aspects and performance evaluations [12].

Several scholars have undertaken performance comparisons between solar photovoltaic-powered and conventionally electrically powered water pumping systems, such as grid and diesel generators, in rural contexts. Their aim has been to minimize water pumping costs while conserving energy [13-19].

In the pursuit of optimal solar PV water pumping system designs, some researchers have utilized simulation software to meet specific requirements through streamlined design optimization approaches [20-23]. Addressing the dynamic challenges arising from changing water demand throughout the irrigation season and varying solar irradiation, [24] developed simulation tools to achieve successful and cost-effective designs. In the context of irrigation-focused solar PV systems, a cost-effective sizing methodology has been proposed by [25], who contextualized their findings within the Chilean scenario and extended the potential applicability to other Latin American nations. The work of [26] explored novel ways to enhance PV system performance, specifically by spraying water on PV cells, resulting in promising outcomes.

Drawing insights from research conducted within Saudi Arabia, numerous studies have examined desalination performance, system sizing, comparative analysis, and influential factors. These studies collectively acknowledge Saudi Arabia's geographical advantage for the installation of photovoltaic (PV) systems in remote or rural regions. The viability of employing a PV water pumping system to ensure consistent access to quality water throughout daylight hours has been substantiated in the context of water desalination plants [27-28]. Almarshoud's work includes a case study involving the sizing of a PV water pumping application, using the shortest sunny day as a parameter in Buraydah city within the Al Qassim Region [29].

A notable instance of optimization arises from a comparative study conducted across diverse geographical locations within Saudi Arabia, evaluating the effectiveness of solar photovoltaic power systems versus diesel generators. The findings align with the ambitions of the 2030 vision and exhibit promising outcomes [30]. In another vein, [31] delve into the determination of optimal PV array configurations, focusing on an effect factor—pumping head. Their investigation, conducted in Al Madinah, contrasts four pumping heads under sunny conditions, ultimately identifying the most efficient configuration.

This study aims to achieve the optimal design for a water pumping system that harnesses solar energy and utilizes available water resources in six distinct regions within the kingdom, with the primary objective of meeting water demand at the lowest possible cost. Additionally, it seeks to conduct a comparative analysis of the utilization of solar energy in lieu of the utility grid for both standalone PV systems and grid-connected PV systems. Furthermore, the study will involve the calculation of key economic indicators for the proposed system, including the Levelized Cost of Produced Water, the Levelized Cost of Generated Energy, and the Payback Time.

II. Study Area

The Kingdom of Saudi Arabia stands out as a country endowed with significant agricultural potential. Despite being predominantly arid, it boasts multiple agricultural regions with abundant fertile lands. Notable examples include Al Ahsa governorate, Ha'il region, Al Jouf region, Al Qassim region, Al Kharj governorate, and Wadi Aldoaser governorate. Furthermore, the kingdom is blessed with numerous aquifers that contain ample reserves of freshwater. Additionally, the kingdom's strategic geographical location ensures it receives ample solar energy radiation. For instance, in the region with the lowest solar radiation levels [32], the average still reaches an impressive 2000 kWh/m2. Table 1 provides a summary of the key features and characteristics of these selected regions.

Table (1): The key features and characteristics of these selected regions; [32].

Region	Location	Average Ambient Temperature (^{o}C)	Range of Global Horizontal Irradiance (kWh/m^2 per month)	The annual cumulative of Global Horizontal Irradiance (kWh/m^{2}per year)
Al Ahsa	49^{o}36' E & 25^{o}23' N	27.43	123.22-216.68	2064.07
Ha'il	41^{o}72' E & 27^{o}51' N	24.32	113.48-243.06	2146.49
Al Jouf	39^{o}30' E & 29^{o}30' N	22.23	107.37-251.53	2168.96
AlQassim	42^{o}52'E & 25^{o}48'N	26.14	111.11-240.79	2129.28
Alkharj	47^{o}18' E & 24^{o}08' N	26.68	131.12-225.38	2152.22
Wadi Aldoaser	44^{o}47' E & 20^{o}27' N	28.15	152.83-222.13	2271.68

III. Research Methodology

For evaluating the technical and economic performance of pumping systems under study, a methodology of six steps will be followed; i) specifying the primary data, ii) calculating insolation on a tilted surface, iii) sizing the pumping system, iv) sizing the PV array, v) calculating the technical performance indicators, and vi) calculating the economic feasibility indicators.

Usually, the available solar radiation data for a certain location included the Global Horizontal Irradiance (GHI) which should be converted into tilted surface values at a chosen tilt angle. This transformation process to tilted surface values is a complicated mathematical method. A lot of models for transposition between the horizontal and tilted planes were suggested in the literature, some of the commonly used transposition models were developed by (Hay, 1979; Klucher, 1979; Skartveit&Olseth, 1986; Perez et al, 1990; Reindl et al, 1990; Duffie & Beckman, 1990; Muneer, 2007; Thevenard& Humphries, 2005; Gueymard, 2008; Liu & Jordan, 1963). These models are different in properties and accuracy based on the input data used. Fortunately, these models are available in some computer packages such as HONOR, RETScreen, etc. and they are functional to convert GHI to tilted values at any desired tilt angle.

In the present study, the RETScreen has been used for converting GHI values to tilted surface. RETscreen adopts a simple isotropic model of diffuse radiation which presented by Liu and Jordan (1963) [33], this model is considered simple and accurate especially in the clear sky case. The Liu and Jordan model is as follows:

$$G_t = G_{dn}\cos\theta + G_d R_d + \mu G R_r \qquad (1)$$

Where Gt is the global irradiance on the tilted plane, Gdn is the direct normal irradiance (DNI), Gd is the diffuse irradiance on the horizontal plane (DHI), G is the global horizontal irradiance (GHI), θ is the angle of the sun ray on the tilted plane, Rd is the transposition factor of diffuse radiation, μ is the foreground's albedo, and Rr is the transposition factor of ground reflection.

Because the available solar irradiance data are based on the total potential energy per day, therefore, the estimation of the energy needed by the motor-pump system should also be calculated depending on the total daily demand of water according to the following formula [29]:

$$\mathrm{E_{pump}\ (Wh)} = \frac{\rho g Q H}{3.6\,\eta_m\,\eta_p} \qquad (2)$$

Where: *H* is the Total Dynamic Head (TDH) which is the sum of the static head of water in the well, discharge head, drawdown head, discharge pressure and friction loss in the pipeline, ρ is the density of water (1.0 kg/L), g is the gravity acceleration (m/sec^2), Q is the daily demand of water (m^3), η_m is the motor efficiency and ηp is the pump efficiency.

The daily output energy of PV array may be given by the following formula [34]:

$$E_{pv}(Wh) = A_{pv}\,\bar{G}_t\,\eta_{pv}(1-\lambda_m)(1-\lambda_c) \qquad (3)$$

Where $\bar{G}_t$ is the global solar insolation on the tilted surface (W/m^2/day), $A_{pv}$is the area of the PV array (m^2), η_{pv} is the efficiency of PV array under operating condition, $\lambda_{m,}$ and λ_c are miscellaneous losses of PV array and power conditioning losses respectively, usually the values of $\lambda_{m,}$ and λ_c assumed from 1- 2 % for each.

The sizing of PV array could be done by matching the total energy needed daily by the motor-pump system with the daily expected output energy of PV array as in the following

From eqns. 2 & 3

$$E_{pv}\,(Wh) = \mathrm{E_{pump}}\ (\mathrm{Wh}) \quad (4)$$

Because the motor-pump is connected to the PV array through the inverter, then Eqn. 4 could be modified as follows:

$$E_{pv} = \frac{E_{pump}}{\eta_{inv}} \quad (5)$$

$$A_{pv}\,\bar{G}_t\,\eta_{pv}(1-\lambda_m)(1-\lambda_c) = \frac{\rho g Q H}{3.6\,\eta_m\,\eta_p\,\eta_{inv}} \quad (6)$$

Where η_{inv} is the efficiency of the inverter. Then the size of the PV array needed for the water pumping system could be obtained as follows:

$$A_{pv} = \frac{\rho g Q H}{3.6\,\bar{G}_t\,\eta_{pv}\eta_m\,\eta_p\,\eta_{inv}\,(1-\lambda_m)(1-\lambda_c)} \quad (7)$$

The value of η_{pv} could be obtained as [34]:

$$\eta_{Pv} = \eta_r\ [\,1 - \alpha_p\,(\,T_c - T_r\,)\,] \quad (8)$$

Where η_r is the PV module efficiency at the reference cell temperature at STC (T_r = 25°C), and α_p is the temperature coefficient for module efficiency. While, T_c is the cell temperature. For the average ambient temperature, T_a can be calculated as follows[35]:

$$\mathrm{T_c} - \mathrm{T_a} = \frac{(\mathrm{NOCT}-20)}{800} G_t \quad (9)$$

Where NOCT is the Nominal Operating Cell Temperature, and G_t is the global irradiance incident on the tilted plane in (W/m^2).

The technical performance of a PV water pumping system relies on International Energy Agency (IEA) indicators, emphasizing the consumed energy by the pumping system over PV array generation. Key indicators encompass Energy yield, Yield Factor, Capacity Factor, and Performance Ratio.
Energy Yield (EY) is the absorbed energy by the pumping system, while Yield Factor (YF) gauges PV array productivity under specific weather conditions. YF is calculated as the ratio of consumed energy by the pumping system (annual, monthly, or daily) to the peak power of the PV array at standard test conditions (STC) and it is given as follows [36]:

$$\mathrm{YF} = \frac{\mathrm{E_{Consumed}}\ \ (\mathrm{kWh\ /year\ })}{\mathrm{PV_{array}}\ (\mathrm{kW_{peak}}\ )} \quad (10)$$

Capacity Factor (CF) assesses PV system usability, calculated as the ratio of actual consumed energy to the energy the PV system would generate if it works at its full capacity for 24 hours per day all the year. Ideal CF will not be more than 50% since the sun is available only about half the day. Typical CF, often around 40% globally, accounts for energy conversion losses and climate change. The CF is calculated as the following [37]:

$$\boldsymbol{CF} = \frac{\mathrm{E_{Consumed}}\ \ (\mathrm{kWh\ /year\ })}{\left(8760 * \mathrm{PV_{array}}\ (\mathrm{kW_{peak}}\ )\right)} \quad (11)$$

or $$\boldsymbol{CF} = \frac{\boldsymbol{YF}}{\boldsymbol{8760}} \quad (12)$$

Performance Ratio (PR) is defined as the real amount of PV energy delivered to the pumping system in a certain period divided by the output rated energy according to the STC data of the modules [37]. PR is independent of location or system size, because it indicates the overall effect of losses on the array's nominal power as a result

for; wiring mismatch, inverter inefficiency, PV module temperature, incomplete use of insolation, soiling or snow, component failures, and system downtime [38-39].

$$PR = YF \cdot G_{STC} / \sum \bar{G}_t \quad (13)$$

Where G_{STC} is the irradiance at STC, and $\sum \bar{G}_t$ is the accumulative irradiance on the plane of PV array within a certain period (annual, monthly, or daily).

Economic feasibility is assessed via three indicators: Levelized Cost of Generated Energy (LCOE), representing average energy cost ($/kWh) during the PV system's life cycle; Levelized Cost of Produced Water (LCOW), denoting average water cost ($/m^3); and Simple Payback Time (SPBT).LCOE is the Life Cycle Cost (LCC) of the PV pumping system divided by the amount of expected generated energy during the project life cycle. LCC sums all PV water pumping system expenses over its life cycle, adjusted to present-day value, considering the effect of time on the value of money [40]. This approach brings future expenses to current-year costs through discounting. The life cycle cost is given as following [41]:

$$LCC = C_{capital} + \Sigma\, C_{O\&M} + \Sigma\, C_{replacement} - C_{salvage} \quad (14)$$

The capital cost (C_{apital}) of a PV system includes the initial cost of equipment, design of the system, engineering, and installation. The capital cost is always considered as a single payment paid in the first year of the project. The operation and maintenance cost ($C_{O\&M}$) is the sum of all scheduled operation and maintenance costs during the year. The cost of replacement ($C_{replacement}$) is the sum of equipment replacement costs and the cost of all spare parts that anticipated over the life cycle of the project. The salvage value ($C_{salvage}$) is the value of the equipment at the end of its life cycle period. All anticipated expenses should be discounted to the present worth taking into consideration the inflation rate (i) and the discount rate (d).

The Present worth (PW) of any future cost is given by [40]:

$$PW_n = \frac{C(1+i)^{n-1}}{(1+d)^n} \quad (15)$$

Where, ***n*** is the number of years.

Next, include the Levelized cost of energy (LCOE), which can be calculated by dividing the life cycle cost value of the project by the expected generated energy during the project life cycle as follows [23]:

$$LCOE = LCC / \Sigma\, E_{generated} \quad (16)$$

Where the energy generated over the life cycle ($E_{generated}$) would be calculated taking into account the degradation rate of PV modules as following:

$$E_{generated} = \sum_{i=0}^{n-1} E_{1st\ year} \cdot (1 - deg\%)^i \quad (17)$$

Where: n is the total project years, deg% is the percentage of annual degradation in output energy, $E_{1st\ year}$ is the energy generated during the 1st year.

The Levelized cost of water (LCOW) can be calculated by dividing the life cycle cost value of the project by the amount of produced water during the project life cycle as follows:

$$LCOW = LCC / \Sigma Q_{Life\_cycle} \quad (18)$$

Moreover, the annual savings will include the avoided cost of energy supplied by the grid in case not using the PV system during the life of project, and it is gotten by:

$$\text{Benefits from avoided energy} = 0.16\ (SR) * 1.15 * E_{Consumed} \quad (19)$$

0.16 SR (0.0427 $) is the electricity energy tariff of the agriculture sector per kilo Watts hour, 1.15 is the added VAT.

Considering the cost of avoided energy as apart of annual savings will reflect positively in reduction of the Simple Payback (SPBT). Additionally, another factor to reduce the recovery period and utilize excess energy involves selling electricity to the Saudi Electricity company grid, though it's not highly encouraged due to the low tariff, priced at 0.05 SR (0.0134 $) per kWh, as documented by the Water & Electricity Regulatory Authority (WERA).

$$\text{Price of Exported Energy} = 0.05(SR) * (E_{expected} - E_{consumed}) \quad (20)$$

The Simple Payback Time (SPBT) is considered one of the most requested indicators of the economic feasibility of renewable energy systems, which calculates the number of years for the savings of energy from the renewable energy project to offset the initial cost of investment and given as the following [42]:

$$SPBT(years) = \frac{Initial\ \ Cost\,(\$)}{\left(Savings: Price\ of\ avoided\ \ energy + price\ of\ exported\ \ energy\ \right)\ \ (\$/year) - C_{O\&M}(\$/year)\right)} \quad (21)$$

IV. Technical Analysis of the Selected Case Studies

4.1 Specifying the primary data

The Global Horizontal Irradiance (GHI) data for the six selected locations was sourced from the SolCast website, a comprehensive platform offering meteorological data based on satellite imaging for global locations [35]. Table (2) provides detailed specifications of the wells under consideration, while Figure (1) visually presents the monthly variations in Global Horizontal Irradiance (GHI) in all regions included in the study. Furthermore, Figure (2) offers a graphical representation of the monthly fluctuations in daily average ambient temperatures for these regions.

Table 2: The specifications of the wells under consideration

Region	Well No.	Longitude (^{O})	Latitude (^{O})	Height (m)	Depth (m)	TDH* (m)
Al Ahsa	**1**	49.51982	25.42169	158	193	107
Ha'il	**2**	42.56664	27.71716	726	417	168
Al Jouf	**3**	38.308420	29.79748	647	450	214
Al Qassim	**4**	44.11939	26.06588	661	567	126
Al Kharj	**5**	47.21067	24.08112	437	170	110
W. Aldoaser	**6**	44.63524	20.45307	707	300	170

*****The total dynamic head (TDH) of pumping is defined as the total equivalent level (height) of fluid to be pumped, considering (10-20m) as friction losses

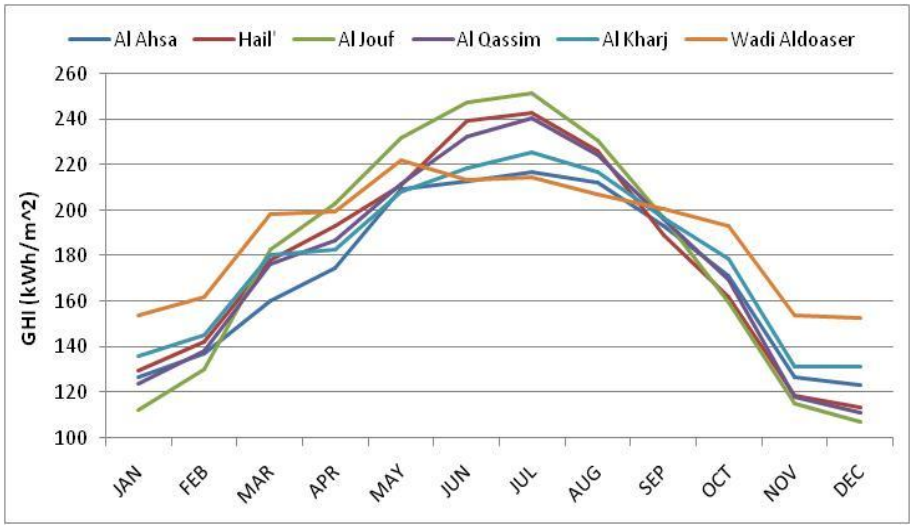

Figure 1: Monthly Variation of GHI

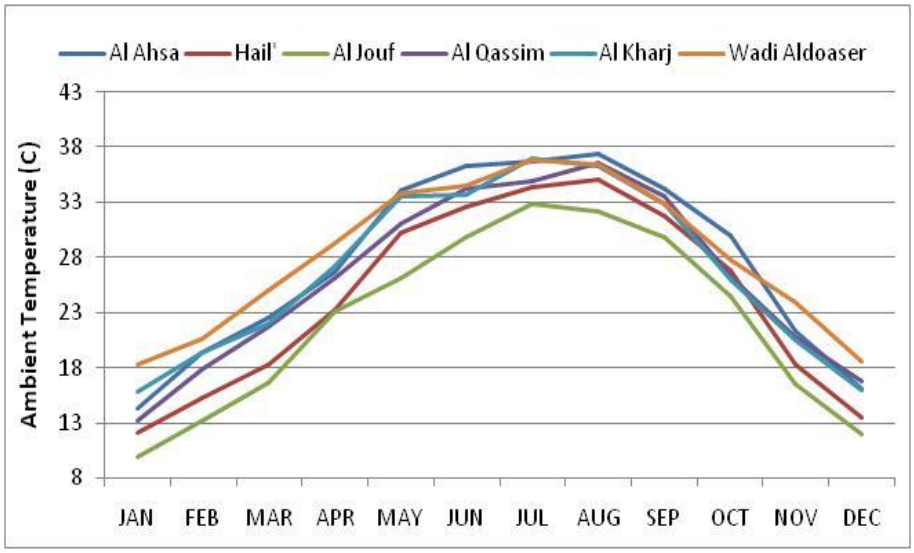

Figure 2: The monthly variation of daily average ambient temperature

4.2 Calculating the Insolation on the Tilted Surface (GTI)

Table (3) demonstrates the values of solar irradiance on the tilted plane (GTI) generated by the RETScreen package in addition to the global solar irradiance on horizontal plane (GHI) for each well.

Table 3: Monthly average of GHI & GTI in (kWh/m^2/day)for all regions under study

Months	Al Ahsa		Ha'il'		Al Jouf		Al Qassim		Al Kharj		Wadi Aldoaser	
	GHI	GTI	GHI	GTI	GHI	GTI	GHI	GTI	GHI	GTI	GHI	GTI
JAN	4.08	5.34	4.19	5.80	3.62	5.15	3.99	5.31	4.39	4.81	4.97	6.07
FEB	4.91	5.91	5.09	6.39	4.64	5.87	4.94	6.04	5.18	5.51	5.78	6.68
MAR	5.16	5.56	5.76	6.38	5.9	6.70	5.7	6.25	5.83	5.77	6.4	6.81
APR	5.83	5.76	6.43	6.39	6.76	6.78	6.22	6.17	6.1	6.11	6.66	6.55
MAY	6.76	6.24	6.8	6.25	7.49	6.84	6.83	6.29	6.71	6.61	7.17	6.65
JUN	7.09	6.31	7.98	6.99	8.24	7.16	7.75	6.84	7.29	6.99	7.11	6.41
JUL	6.99	6.32	7.84	7.00	8.11	7.20	7.77	6.97	7.27	6.85	6.92	6.33
AUG	6.84	6.57	7.29	7.01	7.45	7.19	7.23	6.95	7	6.91	6.69	6.42
SEP	6.43	6.77	6.3	6.70	6.56	7.11	6.53	6.92	6.56	6.77	6.68	6.89
OCT	5.53	6.50	5.22	6.26	5.15	6.38	5.47	6.51	5.77	6.37	6.23	7.04
NOV	4.22	5.38	3.96	5.22	3.85	5.32	3.94	5.06	4.37	5.31	5.13	6.24
DEC	3.97	5.37	3.66	5.14	3.46	5.13	3.58	4.85	4.24	4.51	4.93	6.24
Annual Average	5.65	6	5.88	6.29	5.94	6.40	5.83	6.18	5.89	6.04	6.22	6.53

4.3 Sizing the motor-pump system

Table (5) outlines estimated motor-pump system sizes, with actual ratings subject to local market availability. A market survey guided the selection of Grundfos as the preferred brand. Subsequently, three sizes of Grundfos pumping systems, chosen based on the initial ratings in Table (4), are detailed in Table (5), while their technical specifications are shown in Table (6). Inverters, sized to match the motor-pumping system, are specified in Table (7).

Table 4: Sizing of motor-pump system

	Al Ahsa	Ha'il	Al Jouf	Al Qassim	Al Kharj	Wadi Aldoaser
	Well (1)	Well (2)	Well (3)	Well (4)	Well (5)	Well (6)
TDH (m)	107	168	215	126	110	170
Minimum Power rating (kW)	16.19	25.41	32.50	19.10	16.64	25.77

Table 5: Selected sizes of pumping system from Grundfos Co.

	Al Ahsa	Ha'il'	Al Jouf	Al Qassim	Al Kharj	Wadi Aldoaser
	Well (1)	Well (2)	Well (3)	Well (4)	Well (5)	Well (6)
Rated TDH (m)	171	205	275	171	171	205
Selected Power rating (kW)	22	30	37	22	22	30

Table 6: *Motor-pump system specifications*

Pump			
Brand Name	Grundfos		
Type	Multi-stage, submersible		
Model	150S300-15	150S400-18	150S500-24
Rated Head (m)	171	205	275
Efficiency (%)	70.6		
Rated Flow (m^3 /hour)	34		
Speed (rpm)	3450		
Motor			
Model	MS6000QFT30	MS6000QFT40	MS6000QFT50
Output Power (kW)	22	30	37
Efficiency (%)	85	86	84
Rated Voltage (V)	3Φ *380		
Rated Current (A)	46	63.5	68.7
Starting Current (A)	238	330	470
Frequency (Hz)	60		
Power Factor (%)	85	84	83

Table 7: Inverter nameplate data

Inverter			
Brand Name	SAKO		
Model	SKI650		
Efficiency (%)	98		
Frequency (Hz)	0 - 60		
Min-Max Input Voltage (V)	350-750 $_{DC}$		
Output Voltage (V)	380 $_{3Φ}$		
The output Rated Power (kW)	22	30	37

Rated Input Current (A)	56	74	94
Rated Output Current (A)	44	60	74

4.4 Sizing of the PV array

A good quality PV module from (JA solar) has been selected from local market to be used in all cases under investigation. Table (8) shows the key specifications of the selected module.

Table 4: PV module nameplate data

PV Module	
Brand Name	JA Solar
Type	JAM72S30
Rated Maximum Power (W)	545
Dimension (mm)	2278 * 1134
Module Efficiency (%)	21.1
Cell type	Mono-Crystalline silicon
Temperature Coefficient of Pmax	-0.35 %/^{o}C
NOCT (^{o}C)	45±2^{o}C
Maximum Voltage (V)	41.8
Maximum Current (A)	13.04
Open Circuit Voltage (V)	49.75
Short Circuit Current (A)	13.93

Data of PV module measured at STC (GHI: 1000 w/m^2, air mass: 1.5 g, Cell Temperature: 25^{o} C)

The PV module's efficiency, initially measured in STC, required recalculations for different climate conditions. The method outlined in section 3 was applied, yielding new module efficiency values displayed in Table (9) for each case study's climate conditions.

Table 5: New values of PV Moduleefficiency based on the climate condition of each case study

	Al Ahsa	Ha'il'	Al Jouf	Al Qassim	Al Kharj	W. Aldoaser
	Well (1)	Well (2)	Well (3)	Well (4)	Well (5)	Well (6)
Efficiency (η_{pv})	18.75	18.81	18.91	18.70	18.80	18.52

Using the pumping system's energy demand and case study solar irradiance, PV array sizes were determined, applying the method from section 3 with updated efficiency values from Table (9). Table (10) displays the resulting PV array sizes for each well.

Table 6: The PV array size for all wells under study

	Al Ahsa	Ha'il'	Al Jouf	Al Qassim	Al Kharj	W. Aldoaser
	Well (1)	Well (2)	Well (3)	Well (4)	Well (5)	Well (6)
Number of PV modules	38	56	70	44	40	56

Following the determination of the appropriate PV array size for each well, two tests were conducted to assess its energy supply capabilities: firstly, a year-round evaluation to analyze the impact of solar irradiance fluctuations, particularly during winter months, involved a monthly comparison of expected energy generation with consumption for all wells throughout the year, as depicted in Figure (3). The results revealed the PV array's inability to meet energy demands during winter months across all wells, except for well 6 in the Wadi Aldoaser region. Secondly, a long-term

evaluation examined the PV array's performance over its 25-year life cycle, accounting for typical PV cell degradation. A yearly comparison of expected energy generation and consumption was carried out for all wells, considering PV module degradation, as illustrated in Figure (4). These results indicated that, after year 17, most wells failed to consistently supply adequate energy throughout the PV array's life cycle, except for well No. 5. To address these limitations and enhance PV array performance in the face of low winter irradiance and degradation effect, three solutions were proposed: 1) increasing the PV array size, 2) adjusting the tilt angle of PV array, and 3) Using a one-axis tracking system.

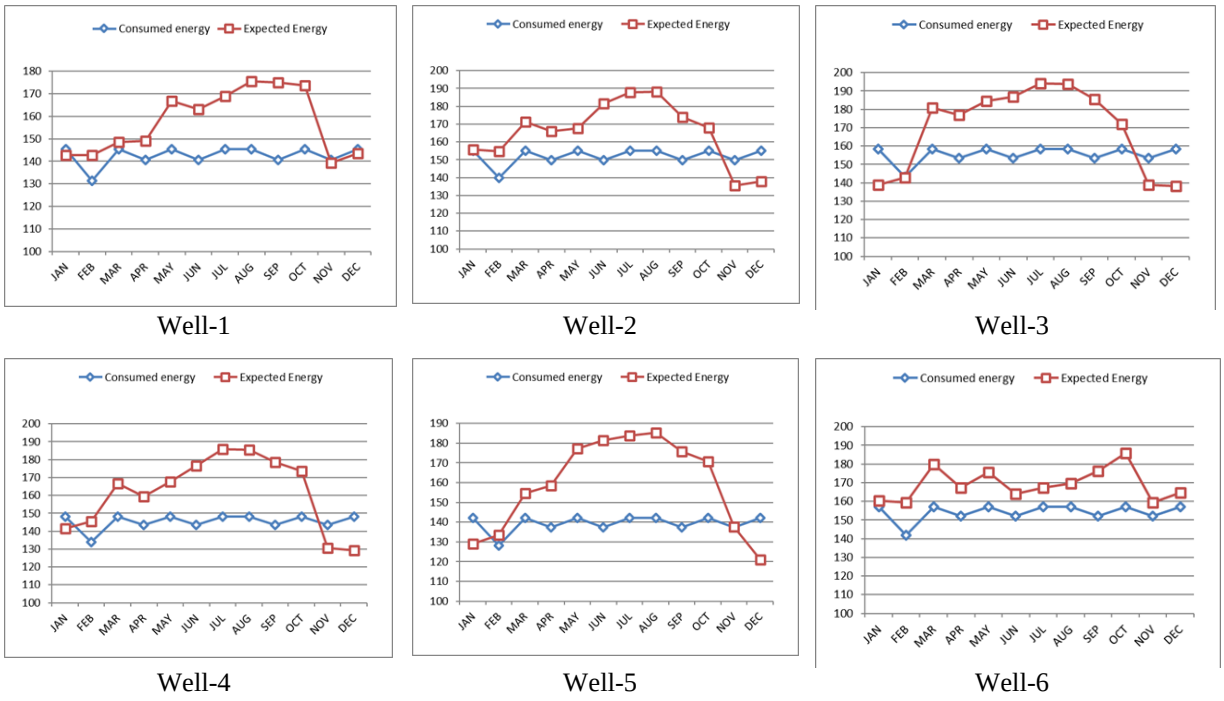

Figure 3: Variation of expected and consumed energy represented by Yield Factor during the year

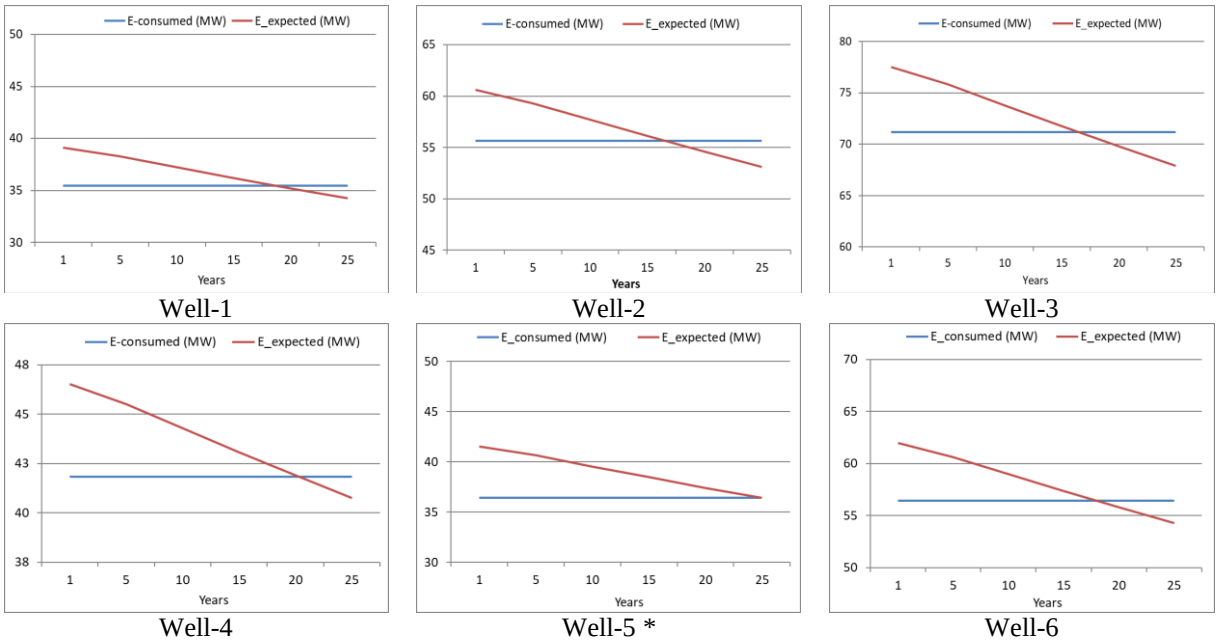

Figure 4: Comparing annual expected and consumed energy for all 6 wells over the system's life cycle, accounting for degradation as a measure of overall energy production losses in PV array performance.

4.4.1 Increasing the size of PV array

This solution involves a gradual increase in the PV system's size to mitigate the mentioned drawbacks. Despite space and other disadvantages, it proved effective by addressing basic design flaws, adding four solar panels to wells 1 and 6, and 8 to 14 extra panels to the remaining wells as indicated in Table (11). Simulation results in Figure (5) reveal that expected energy exceeds consumption annually, while Figure (6) demonstrates the system's ability to overcome annual degradation, consistently meeting energy demand over the PV system's life cycle. Capacity Factor (CF) and Performance Ratio (PR), assessing PV system usability and losses, are calculated for both standalone and grid-connected scenarios, presented in Figures (7) & (8).

Table 7: Comparison of PV array size for both main design and the proposed solution

	Al Ahsa	Ha'il'	Al Jouf	Al Qassim	Al Kharj	W. Aldoaser
	Well (1)	Well (2)	Well (3)	Well (4)	Well (5)	Well (6)
Main number of PV modules	38	56	70	44	40	56
Proposed number of PV modules	42	66	82	52	48	60

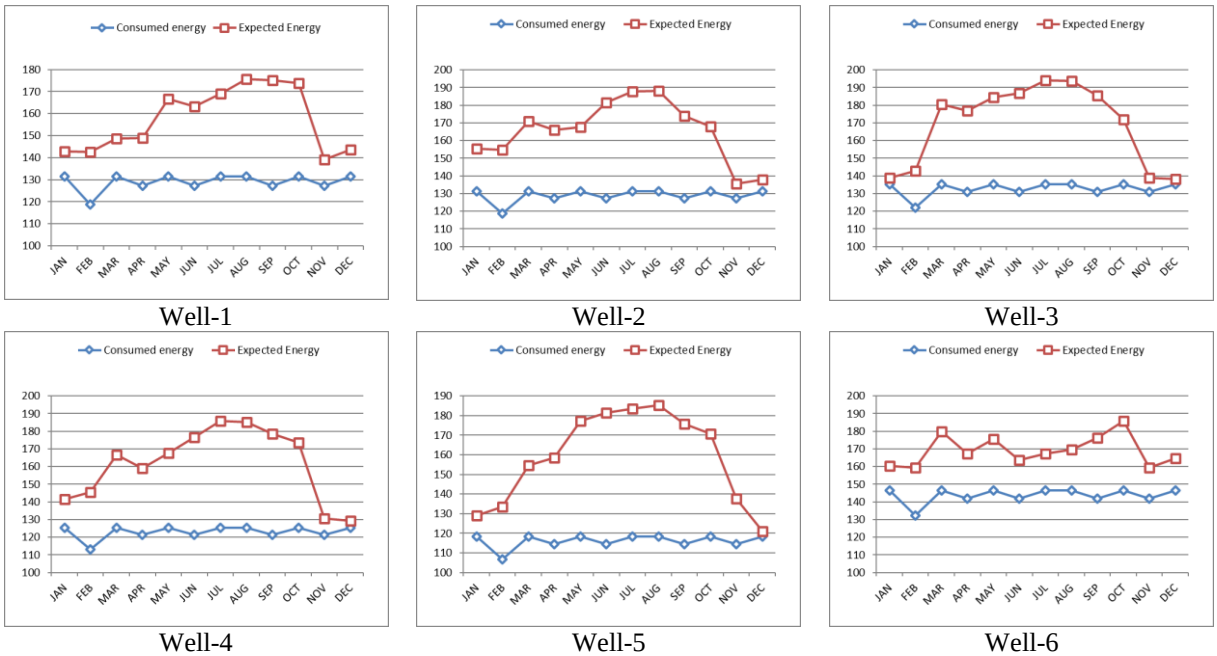

Figure 5: Variation of expected and consumed energy represented by Yield Factor during the year after increasing the size of PV array

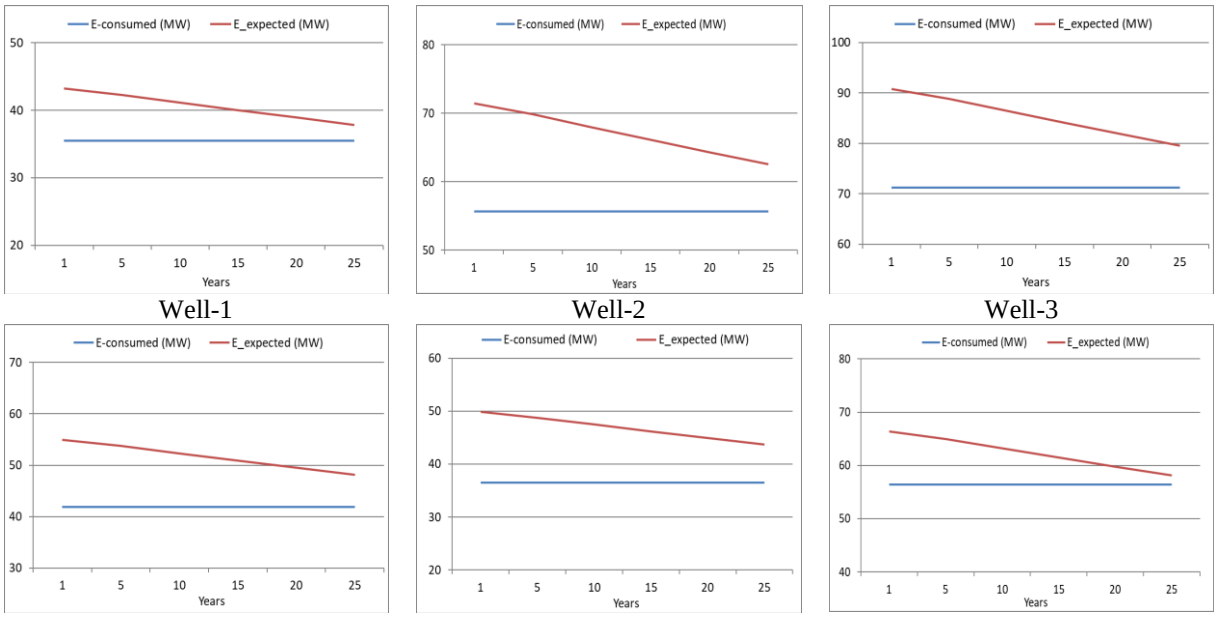

Figure 6: Comparing the annual expected and consumed energy along the life cycle of the system considering the degradation effect

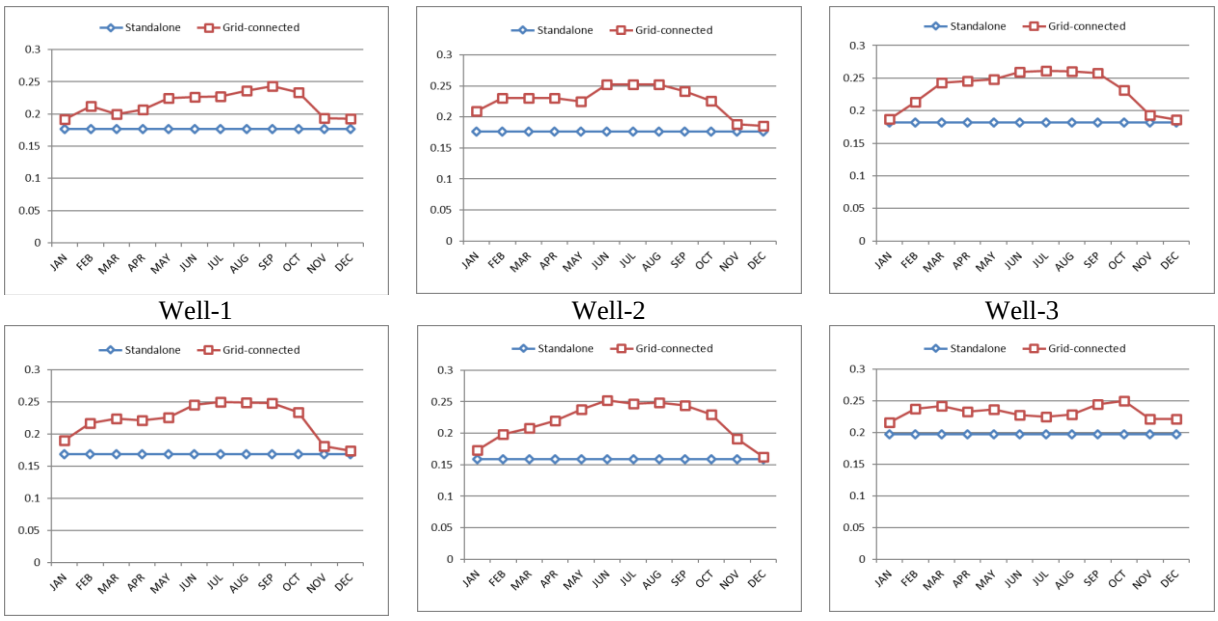

Figure 7: Capacity Factor (CF) after increasing the size of PV array for both stand-alone and grid-connected cases.

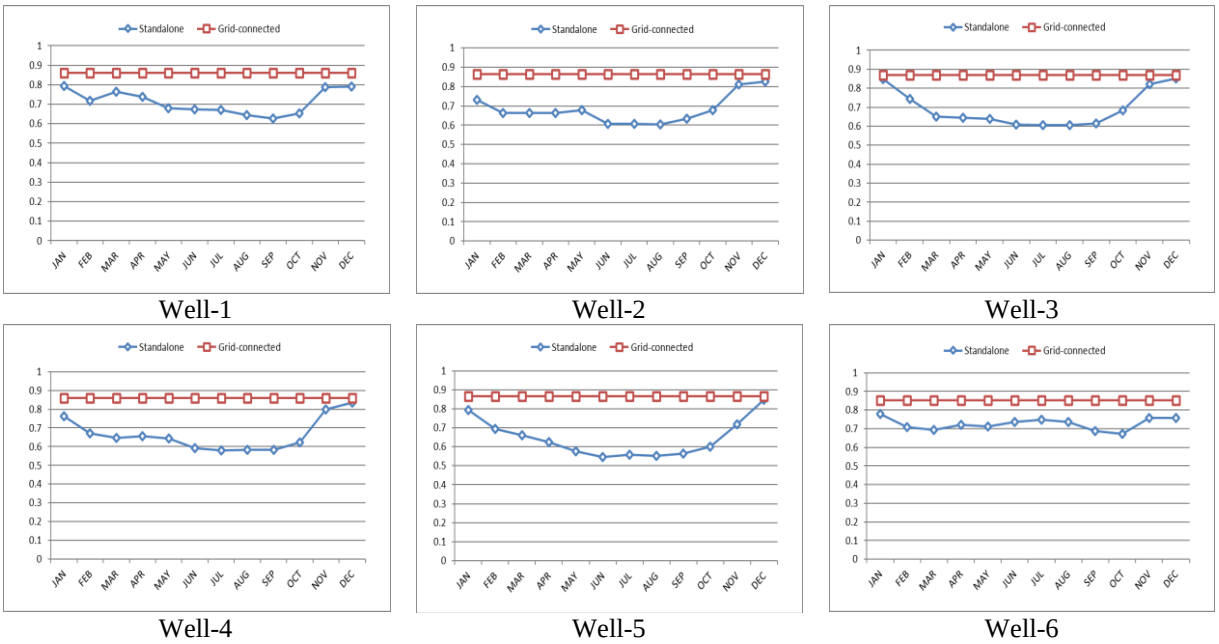

Figure 8: Performance Ratio (PR) after increasing the size of PV array for both stand-alone and grid-connected cases

Figure (5) shows a notable disparity between expected and consumed energy, particularly in summer months, across all wells except 1 and 6 in Al-Ahsa and Wadi Al-Doaser regions. This discrepancy is attributed to increased panel numbers and higher summer solar radiation. In Figure (6), all wells effectively counter degradation, with minor impact observed in wells 1 and 6. The remaining wells demonstrate significant resilience, primarily due to added modules.

Figure (7) displays Capacity Factor in both standalone and grid-connected modes, remaining stable throughout the year in standalone mode (16-20% based on location). In grid-connected mode, it varies (16-26%) with monthly solar radiation rates. Figure (8) illustrates Performance Ratio in both modes. In grid-connected mode, PR remains constant (85-88%) based on location. In standalone mode, PR fluctuates (55-87%) in response to monthly solar radiation changes.

4.4.2Increasing the tilt angle of PV modules

This solution involved increasing the degree of tilted modules by 15 degrees to maximize solar radiation absorption and compensate for reduced winter radiation quality. This adjustment yielded a notable increase, with an average of 1.1 kWh/m2/d. It proved effective across all regions, as indicated in Table (12). Figure (9) demonstrates expected energy consistently exceeding consumption throughout the year, while Figure (10) shows the solution's ability to overcome annual degradation, ensuring energy generation over the PV system's life cycle. Capacity Factor (CF) and Performance Ratio (PR), assessing PV system usability and losses, were calculated for both standalone and grid-connected scenarios, presented in Figures (11) & (12).

Table 8: GTI calculated at tilt angle equals to location latitude plus 15^{o}

	Al Ahsa	Ha'il'	Al Jouf	Al Qassim	Al Kharj	W. Aldoaser
	Well (1)	Well (2)	Well (3)	Well (4)	Well (5)	Well (6)
GTIat tilt angle = latitude	6	6.29	6.4	6.18	6.04	6.53
GTIat tilt angle = latitude+15^{o}	7.05	7.43	7.62	7.33	7.25	7.39

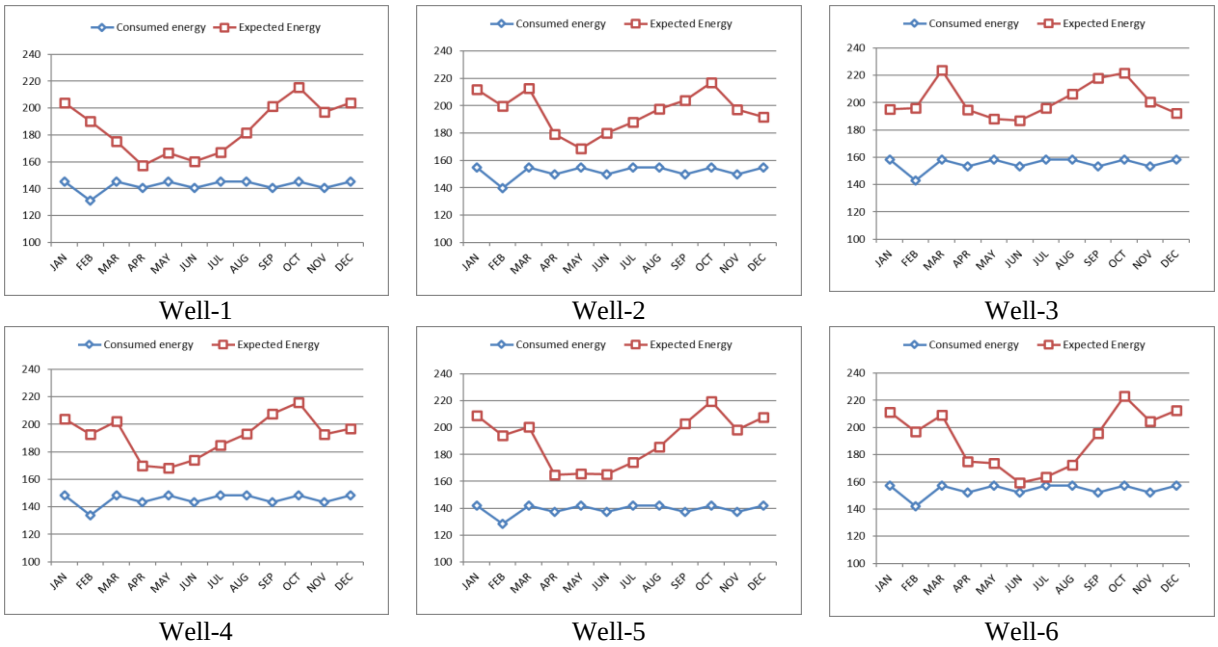

Well-1 Well-2 Well-3

Well-4 Well-5 Well-6

Figure 9: Variation of expected and consumed energy represented by Yield Factor during the year after increasing the tilt angle of PV array by 15^{o}

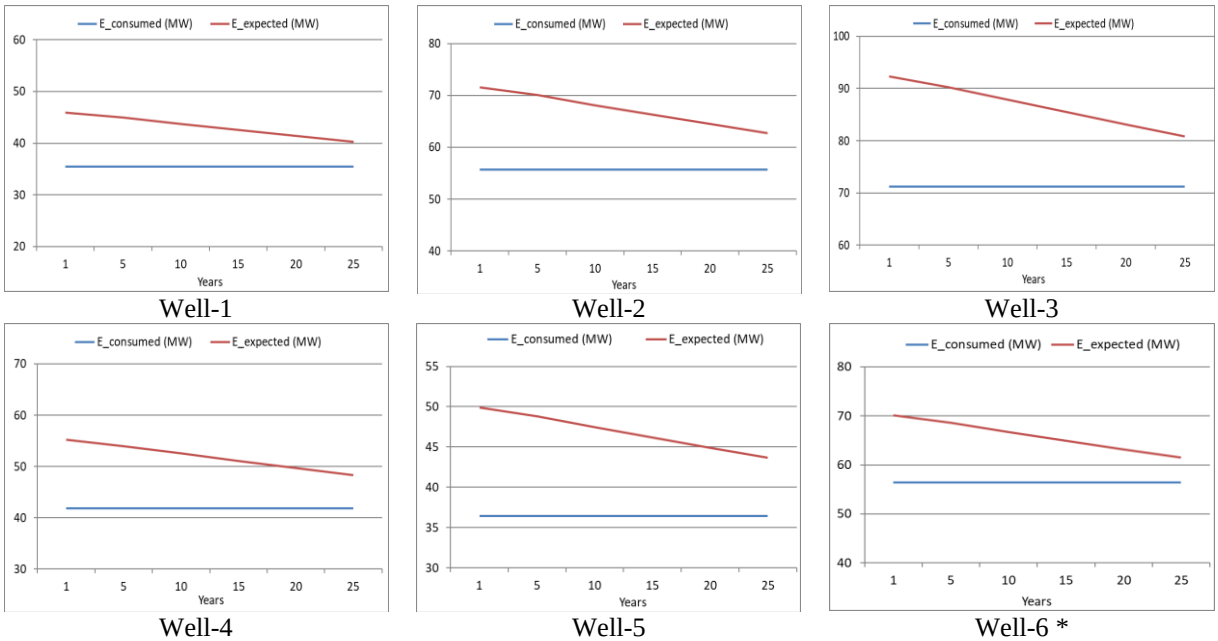

Well-1 Well-2 Well-3

Well-4 Well-5 Well-6 *

Figure 10: Comparing the annual expected and consumed energy during the life cycle after increasing the tilt angle of PV array by 15^{o}

Figure 11: Capacity Factor (CF) after increasing the tilt angle of PV array by 15^{o}

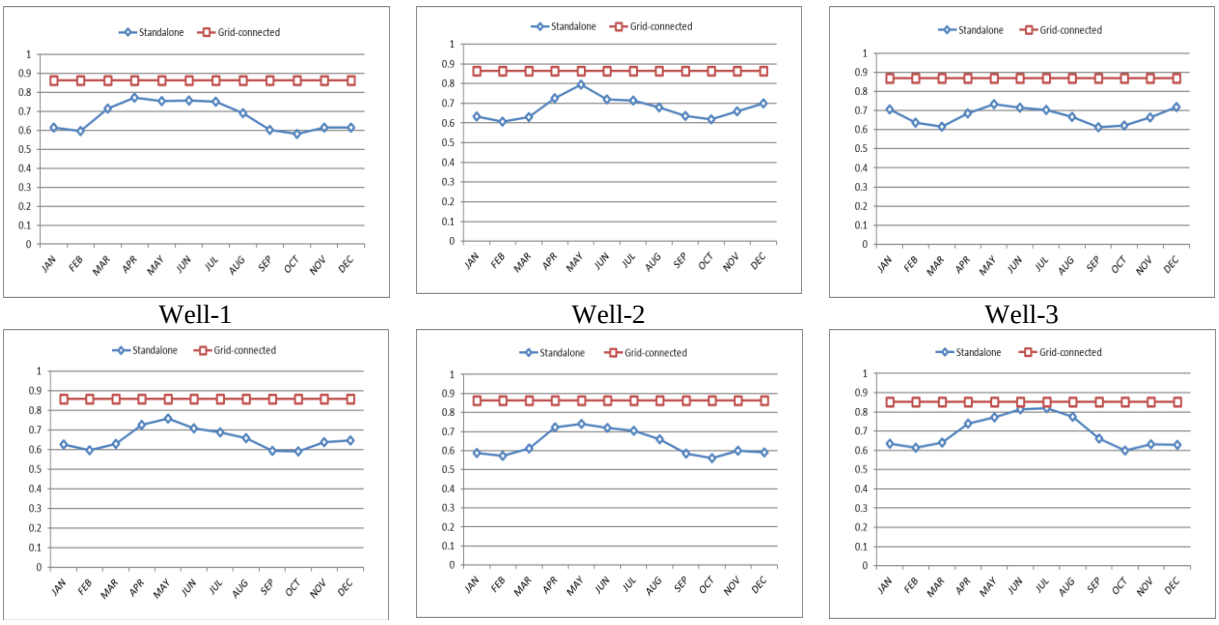

Figure 12: Performance Ratio (PR) after increasing the tilt angle of PV array by 15^{o}

Figure (9) reveals differences between expected and consumed energy, particularly in summer months, for all wells except well 1 in Al Ahsa region andwell 6 in Wadi Al-Doaser region, where the gap may approach zero. Notably, a significant difference occurs in winter months due to the 15-degree tilt increase, enabling the system to generate required energy without size augmentation. In Figure (10), all wells effectively counter annual degradation, with slight margin in well 1 and well6 and substantial margins in the others as a result for increasing the solar system production capacity during winter.

Figure (11) depicts Capacity Factor (CF) in standalone and grid-connected modes. In standalone mode, CF remains fixed throughout the year (19-22% based on location). In grid-connected mode, CF varies (23-30%) in response to monthly solar radiation rates, these values highlight the performance quality of this solution over the first

proposal. Figure (12) illustrates Performance Ratio (PR) in both modes. In grid-connected mode, PR remains constant (86-88%) based on location, while in standalone mode, PR fluctuates (60-82%) based on monthly solar radiation variations.

4.4.3Using one-axis tracking system

In the third proposal, an advanced automated one-axis solar tracking system was employed to optimize solar radiation capture throughout the day, addressing disadvantages such as high installation costs and ongoing maintenance. Nevertheless, it demonstrated significant improvements in system performance during winter months and overcoming annual degradation in all regions. Table (13) presents the updated solar radiation values, while simulation results in figure (13) reveal greater expected energy production than consumption throughout the year. Figure (14) demonstrates the system's ability to combat annual degradation and generate the required energy over the PV system's expected life. Capacity Factor (CF) and Performance Ratio (PR) calculations for both standalone and grid-connected cases are shown in figures (15) & (16) respectively.

Table 9: GTI calculated with using one-axis tracker

Wells number	Al Ahsa	Ha'il'	Al Jouf	Al Qassim	Al Kharj	Wadi Aldoaser
	Well (1)	Well (2)	Well (3)	Well (4)	Well (5)	Well (6)
GTIat fixed tilt angle	6	6.29	6.4	6.18	6.04	6.53
GTIone-axis tracker	7.77	8.33	8.64	8.12	8.14	8.52

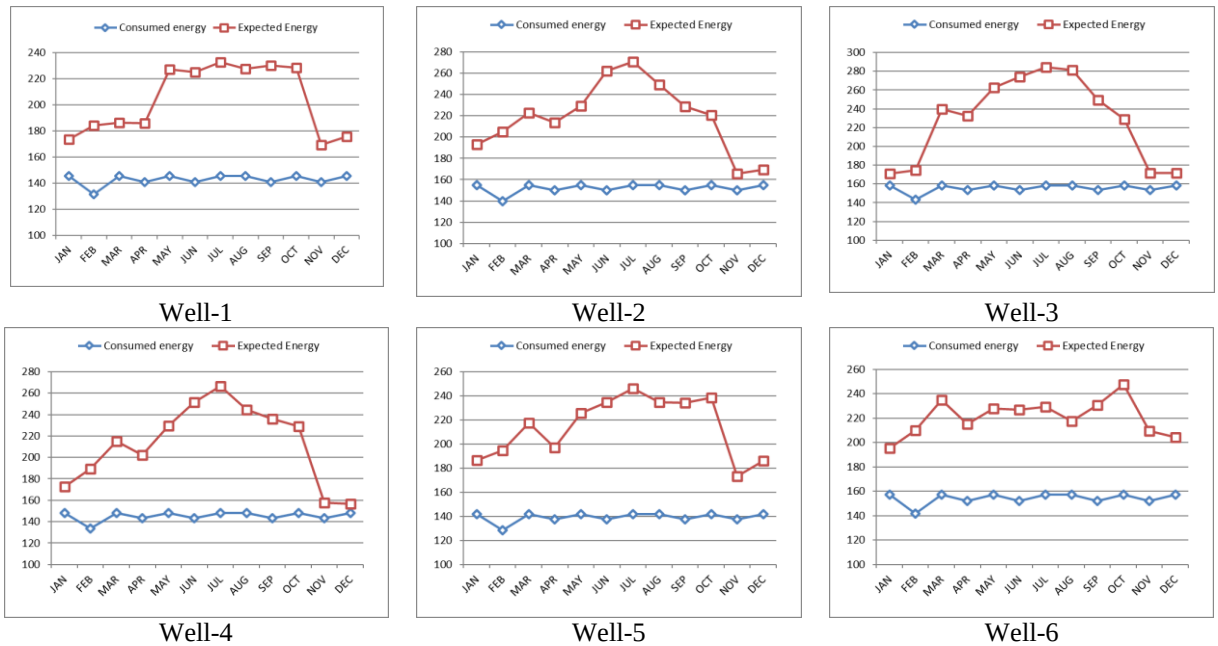

Figure 13: Variation of expected and consumed energy represented by Yield Factor during the year at using one-axis tracking system

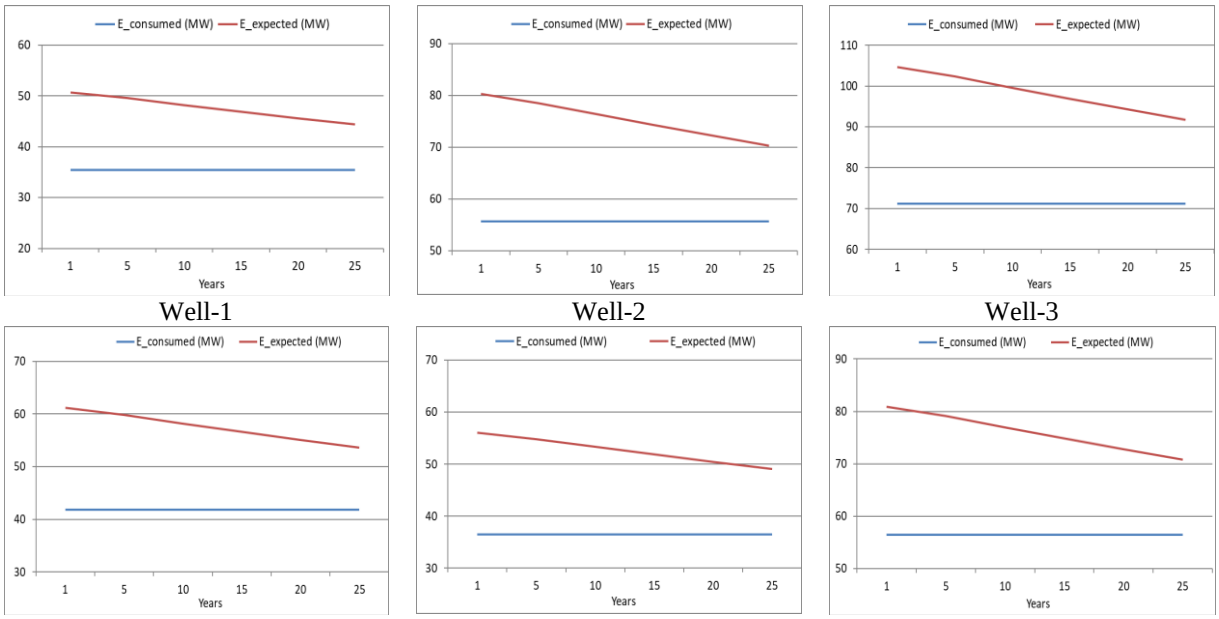

Figure 14: Comparing the annual expected and consumed energy during the life cycle at using one-axis tracking system

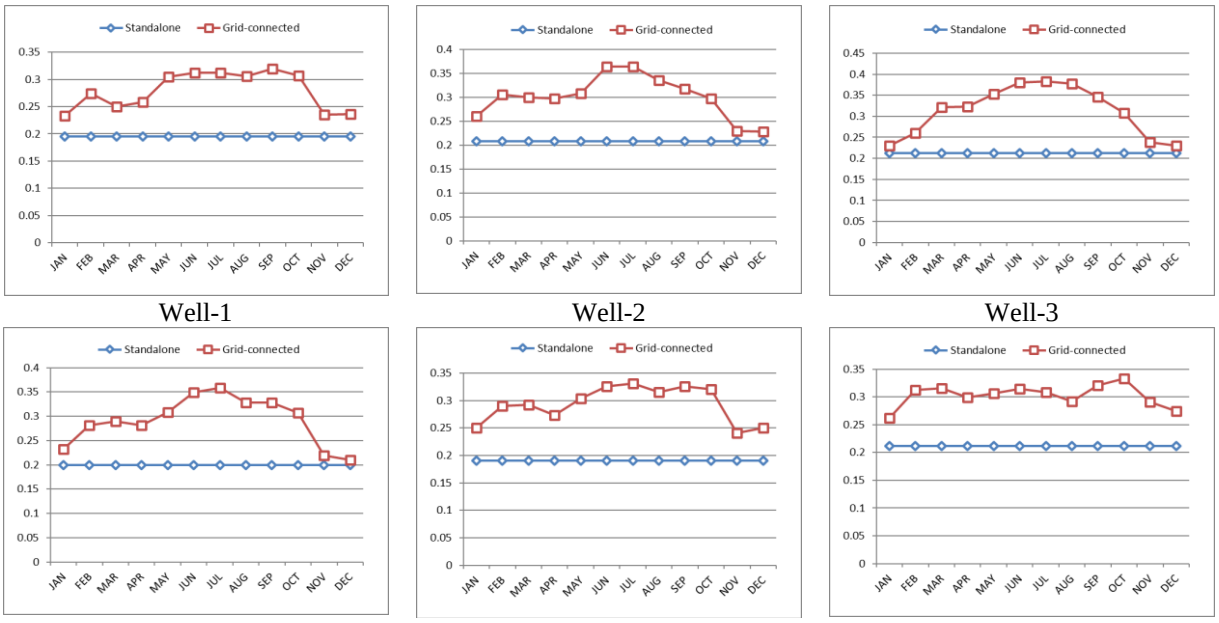

Figure 15: Capacity Factor (CF) at using one-axis tracking system for both stand-alone and grid-connected cases

Figure 16: Performance Ratio (PR) at using one-axis tracking system for both stand-alone and grid-connected cases

In figure (13), there is a significant difference between the expected and consumed energy during summer months, with the expected energy reaching up to 70% of consumed energy. However, this increase is wasteful for standalone systems, negatively impacting performance. In figure (14), all wells effectively overcome degradation, largely due to increased solar system capacity during summer months. Figure (15) displays the Capacity Factor, fixed at 19-22% in standalone mode and variable from 21-38% in grid-connected mode. Figure (16) illustrates the Performance Ratio, fixed at 86-89% for grid-connected systems and variable from 49-80% for standalone systems based on the change in the monthly rate of solar radiation, reflecting significant energy wastage in the latter due to seasonal solar radiation differences with the tracking system.

Tables (14 and 15) display the annual average of Capacity Factor for grid-connected systems and Performance Ratio for standalone systems, facilitating comparison with the main design and proposed options.

Table 10: The annual CF in case of grid-connected operation

No.	Well (1)	Well (2)	Well (3)	Well (4)	Well (5)	Well (6)
Option #1	21.6%	22.7%	23.2%	22.2%	21.8%	23.2%
Option #2	25.4%	26.8%	27.6%	26.3%	26.1%	26.2%
Option #3	27.9%	30.1%	31.3%	29.1%	29.3%	30.3%

Table 11: The annual PR in case of standalone operation

No.	Well (1)	Well (2)	Well (3)	Well (4)	Well (5)	Well (6)
Option #1	71.2%	68%	69.3%	66.4%	64.5%	72.6%
Option #2	67.2%	67.6%	67.3%	65.6%	63.8%	69.4%
Option #3	61.3%	61.3%	61.4%	60.6%	57%	59.7%

It's challenging to discern the superior performance among the three proposed solutions, as it largely depends on the system's mode of operation, whether standalone or grid-connected. For grid-connected mode, Performance Ratio (PR) remains consistent across all options, but Capacity

Factor (CF) excels in option 3. In standalone mode, CF is similar for all three options, while PR performs best in option 1. Option 2 demonstrates moderate values for both CF and PR in both operation modes. Therefore, the economic analysis will play a decisive role in selecting the optimal solution.

4.5Economic Evaluation of the Selected Case Studies

For the economic analysis of the PV pumping systems, a life cycle cost (LCC) analysis was conducted, as detailed in section 3. This analysis encompassed various costs like initial, annual, replacement, balance of system (BOS), and operation and maintenance (O&M) costs, which were sourced from the local market in addition to the project salvage value.Additionally, inflation rate, and discount rate were factored into the LCC calculation, all of which are outlined in Table (16).

Table 12: Parameters and values used in LCC analysis

Item	**Price**			**Life Cycle**
PV module	1557 SR/kW			25 yrs.
Inverter	(22kW) 3052 SR	(30kW) 3937 SR	(37kW) 4856 SR	15 yrs.
BOS *	1207 SR/kW			
O & M **	82 SR/kW/yr.			
Feasibility study	2000 SR			
Grid-tied cost	700 SR			
Project Salvage value	20% of initial cost			
Inflation rate	3 %			
Discount rate	9 %			
Energy exported to grid	0.05 SR/kWh			
Energy imported from grid	0.16 SR/kWh			

*: Includes planning, installation cost, switchgear, DC cables, and mounting structure, BOS in case of using one-axis tracking system is increased 20 % more than original.
**: The O&M in case of using one-axis tracking system is estimated by 11 2 SR/kW/yr.

Considering the identified drawbacks in section 4.4, alternative options were assessed to address the main system's inability to generate sufficient energy in winter and over the PV system's life cycle. A Life Cycle Cost analysis was conducted for all three options, and their economic indicators are compared in Table (17) for standalone systems and Table (18) for grid-connected systems to determine the most economical solution.

Table 13: Economic indicators of three options for standalone system

Economic Indicators	Al Ahsa	Ha'il'	Al Jouf	Al Qassim	Al Kharj	Wadi Aldoaser
	Well (1)	Well (2)	Well (3)	Well (4)	Well (5)	Well (6)
Levelized Cost of Water (LCOW), SR/m^3						
Option 1	0.050	0.078	0.096	0.061	0.057	0.071
Option 2	0.046	0.067	0.083	0.053	0.048	0.067
Option 3	0.053	0.078	0.097	0.061	0.056	0.078
Levelized Cost of Energy (LCOE), SR/kWh						
Option 1	0.104	0.102	0.099	0.107	0.114	0.092
Option 2	0.094	0.087	0.085	0.092	0.096	0.086

Option 3	0.110	0.102	0.099	0.107	0.112	0.101
Simple Payback Time (SPBT), year						
Option 1	14.7	14.5	13.8	15.6	17.0	12.5
Option 2	12.9	11.7	11.3	12.5	13.3	11.5
Option 3	16.3	14.6	14.1	15.7	16.9	14.3

Table 14: Economic indicators of the three options for grid-connected system

Economic Indicators	Al Ahsa	Ha'il'	Al Jouf	Al Qassim	Al Kharj	Wadi Aldoaser
	Well (1)	Well (2)	Well (3)	Well (4)	Well (5)	Well (6)
Levelized Cost of Water (LCOW), SR/m^3						
Option 1	0.051	0.077	0.095	0.061	0.056	0.072
Option 2	0.046	0.066	0.081	0.052	0.047	0.066
Option 3	0.052	0.075	0.092	0.059	0.053	0.075
Levelized Cost of Energy (LCOE), SR/kWh						
Option 1	0.092	0.084	0.082	0.086	0.088	0.084
Option 2	0.077	0.071	0.069	0.073	0.074	0.074
Option 3	0.080	0.072	0.068	0.075	0.074	0.072
Simple Payback Time (SPBT), year						
Option 1	14.3	13.6	13.1	14.5	15.5	12.3
Option 2	12.4	11.1	10.7	11.8	12.4	11.1
Option 3	14.6	13.0	12.3	13.8	14.5	12.7

The proper selection of these options lies on the best economic evaluation, the increasing of tilted angle by 15^o values satisfied the best solution for economic feasibility among the three options in both stand alone and grid-connected modes. Table (19) below shows the average economic values of all 6 wells.

Table 159**:** Average economic values of all 6 wells under study

Options	Modes of operation	LCOW, (SR/m^3)	LCOE, (SR/kWh)	SPBT (years)
Option 1	Stand-alone	0.068	0.102	14.6
	Grid-connected	0.068	0.085	13.9
Option 2	Stand-alone	0.060	0.090	12.1
	Grid-connected	0.059	0.072	11.5
Option 3	Stand-alone	0.070	0.105	15.3
	Grid-connected	0.067	0.073	13.4

The economic analysis indicates that Option 2 has the lowest LCOE and LCOW, along with the shortest payback period in both standalone and grid-connected modes. Option 2's advantage stems from its cost-effectiveness, achieved through precise tilt angle adjustment for optimal energy harvesting.

V. Summary and Conclusions

This study investigates the technical and economic aspects of solar water pumping in Saudi Arabia, focusing on key agricultural regions with varying solar radiation, temperatures, and well depths. One well was studied in each region, using data from the Environment, Water, and Agriculture ministry's database and Solcast website. Local market prices informed the cost of PV components. We sized PV pumping systems based on regional parameters and meteorological data, aiming for a daily pumping capacity of 200 m3 per well. Technical analysis revealed energy deficiencies in winter and rapid annual degradation, prompting three solutions: 1) Larger PV arrays, 2) Tilt angle adjustments, and 3) Single-axis tracking systems. We assessed performance with Capacity Factor and Performance Ratio, finding that the second proposed solution (Option 2) demonstrated moderate values across standalone and grid-connected modes for all wells.

After analyzing performance, we evaluated economic aspects using life cycle costing, factoring in the cost of grid-supplied energy. We computed the Levelized Cost of Produced Water, Levelized Cost of Produced Energy, and Payback Period for all three proposed solutions in both operational modes. Option 2 (a 15-degree tilt angle increase) outperformed the others in all economic indicators. It achieved the lowest levelized cost of water and energy, along with the fastest payback period for all wells in both modes. This outcome was anticipated as it incurred no extra costs, merely optimizing the tilt angle. Tailoring the tilt angle for each well individually could yield extra energy, enhancing system performance and economic viability. Consequently, we highly recommend Option 2 for solar pumping applications in Saudi Arabia.

Acknowledgment

Researchers would like to thank the Ministry of Environment, Water, and Agriculture (M. E. W. A.) in the Kingdom of Saudi Deanship for providing the required data about wells under study.

Funding

The authors declare that no funds, grants, or other support were received during the preparation of this manuscript

Competing Interests

The authors declare that they have no known competing financial interests or personal relationships that could have appeared to influence the work reported in this paper.

Availability of data and materials

The datasets generated during and/or analyzed during the current study are included in the manuscript

Reference

[1]. Jones, M. A., Odeh, I., Haddad, M., Mohammad, A. H., & Quinn, J. C. (2016). Economic analysis of photovoltaic (PV) powered water pumping and desalination without energy storage for agriculture. Desalination, 387, 35-45.

[2]. Meah, K., Fletcher, S., & Ula, S. (2008). Solar photovoltaic water pumping for remote locations. Renewable and sustainable energy reviews, 12(2), 472-487.

[3]. Mokeddem, A., Midoun, A., Kadri, D., Hiadsi, S., & Raja, I. A. (2011). Performance of a directly-coupled PV water pumping system. Energy conversion and management, 52(10), 3089-3095.

[4]. Bora, B., Prasad, B., Sastry, O. S., Kumar, A., & Bangar, M. (2017). Optimum sizing and performance modeling of Solar Photovoltaic (SPV) water pumps for

different climatic conditions. Solar Energy, 155, 1326-1338.

[5]. Lal, S., Kumar, P., &Rajora, R. (2013). Performance analysis of photovoltaic based submersible water pump. International Journal of engineering and technology (IJET), 5, 552-560.

[6]. Allouhi, A., Buker, M. S., El-Houari, H., Boharb, A., Amine, M. B., Kousksou, T., & Jamil, A. (2019). PV water pumping systems for domestic uses in remote areas: Sizing process, simulation and economic evaluation. Renewable Energy, 132, 798-812.

[7]. Yahyaoui, I., Atieh, A., Serna, A., & Tadeo, F. (2017). Sensitivity analysis for photovoltaic water pumping systems: Energetic and economic studies. Energy Conversion and Management, 135, 402-415.

[8]. Abdourraziq, S., & El Bachtiri, R. (2016). Optimum design of photovoltaic water pumping system application. International Journal of Energy and Power Engineering, 10(6), 767-773.

[9]. Bouzidi, B. (2013). New sizing method of PV water pumping systems. Sustainable Energy Technologies and Assessments, 4, 1-10.

[10]. Muhsen, D. H., Ghazali, A. B., & Khatib, T. (2016). Multiobjective differential evolution algorithm-based sizing of a standalone photovoltaic water pumping system. Energy Conversion and Management, 118, 32-43.

[11]. Zahab, E. E. A., Zaki, A. M., & El-sotouhy, M. M. (2017). Design and control of a standalone PV water pumping system. Journal of Electrical Systems and Information Technology, 4(2), 322-337.

[12]. GÜNDOĞDU, A., & Bayram, G. Ü. R. E. (2019). Design, Construction and Implementation of Low Cost Photovoltaic Water Pumping System for Agricultural Irrigatin. Balkan Journal of Electrical and Computer Engineering, 7(1), 72-80.

[13]. Maurya, V. N., Ogubazghi, G., Misra, B. P., Maurya, A. K., & Arora, D. K. (2015). Scope and review of photovoltaic solar water pumping system as a sustainable solution enhancing water use efficiency in irrigation. American Journal of Biological and Environmental Statistics, 1(1), 1-8.

[14]. Verma, S., Mishra, S., Chowdhury, S., Gaur, A., Mohapatra, S., Soni, G., & Saket, S. (2021). Solar PV powered water pumping system–A review. Materials Today: Proceedings, 46, 5601-5606.

[15]. Korpale, V. S., Kokate, D. H., & Deshmukh, S. P. (2016). Performance assessment of solar agricultural water pumping system. Energy Procedia, 90, 518-524.

[16]. Abu-Aligah, M. (2011). Design of Photovoltaic Water Pumping System and Compare it with Diesel Powered Pump. Jordan Journal of Mechanical & Industrial Engineering, 5(3).

[17]. Kolhe, M., Kolhe, S., & Joshi, J. C. (2002). Economic viability of stand-alone solar photovoltaic system in comparison with diesel-powered system for India. Energy economics, 24(2), 155-165.

[18]. Al-Smairan, M. (2012). Application of photovoltaic array for pumping water as an alternative to diesel engines in Jordan Badia, Tall Hassan station: Case study. Renewable and Sustainable Energy Reviews, 16(7), 4500-4507.

[19]. Girma, Z. (2017). Techno-economic analysis of photovoltaic pumping system for rural water supply in Ethiopia. International Journal of Sustainable Energy, 36(3), 277-295.

[20]. Rao, M. J. M., Sahu, M. K., & Subudhi, P. K. (2018). PV based water pumping system for agricultural sector. Materials Today: Proceedings, 5(1), 1008-1016.

[21]. Tiwari, A. K., Kalamkar, V. R., Pande, R. R., Sharma, S. K., Sontake, V. C., & Jha, A. (2021). Effect of head and PV array configurations on solar water pumping system. Materials Today: Proceedings, 46, 5475-5481.

[22]. Sharma, R., Sharma, S., & Tiwari, S. (2020). Design optimization of solar PV water pumping system. Materials Today: Proceedings, 21, 1673-1679.

[23]. Kazem, H. A., & Khatib, T. (2013). Techno-economical assessment of grid connected photovoltaic power systems productivity in Sohar, Oman. Sustainable Energy Technologies and Assessments, 3, 61-65.

[24]. Campana, P. E., Li, H., & Yan, J. (2013). Dynamic modelling of a PV pumping system with special consideration on water demand. Applied energy, 112, 635-645.

[25]. Barrueto Guzmán, A., Barraza Vicencio, R., Ardila-Rey, J. A., Núñez Ahumada, E., González Araya, A., & Arancibia Moreno, G. (2018). A cost-effective methodology for sizing solar PV systems for existing irrigation facilities in Chile. Energies, 11(7), 1853.

[26]. Al-Sulaiman, F. A., Hamdullahpur, F., & Dincer, I. (2011). Performance assessment of a photovoltaic water pumping system by spraying water over the front of photovoltaic cells. Renewable energy, 34(1), 91-96.

[27]. Alawaji, S., Smiai, M. S., Rafique, S., & Stafford, B. (1995). PV-powered water pumping and desalination plant for remote areas in Saudi Arabia. Applied energy, 52(2-3), 283-289.
[28]. Alajlan, S. A., &Smiai, M. S. (1996). Performance and development of PV-plant for water pumping and desalination for remote area in Saudi Arabia. Renewable energy, 8(1-4), 441-446.
[29]. Almarshoud, A. F. (2016, June). Sizing of PV array for water pumping application. In 32nd European Photovoltaic Solar Energy Conference and Exhibition, At Munich, Germany.
[30]. Rehman, S., & Sahin, A. Z. (2015). Performance comparison of diesel and solar photovoltaic power systems for water pumping in Saudi Arabia. International Journal of Green Energy, 12(7), 702-713.
[31]. Benghanem, M., Daffallah, K. O., Alamri, S. N., &Joraid, A. A. (2014). Effect of pumping head on solar water pumping system. Energy conversion and management, 77, 334-339.
[32]. Al-Ahmadi, M. E. (2009). Hydrogeology of the Saq aquifer northwest of Tabuk, northern Saudi Arabia. Earth Sciences, 20(1).
[33]. Liu, B. Y., & Jordan, R. C. (1963). The long-term average performance of flat-plate solar-energy collectors: with design data for the US, its outlying possessions and Canada. Solar energy, 7(2), 53-74.
[34]. Muñoz Cervantes, D., Ribeyron, P. J., Harrison, S., Allebe, C., Descoeudres, A., Despeisse, M. & de Wolf, S. (2016). Status of the EU FP7 HERCULES project: what is the potential of n-type silicon solar cells in europe?. In EU PVSEC 2016: proceedings: 32nd European Photovoltaic Solar Energy Conference and Exhibition: 20-24 June 2016: Munich, Germany, ICM-International Congress Center Munich (pp. 331-334). European Photovoltaic Solar Energy Conference and Exhibition (EU PVSEC).
[35]. Solcast – Solar Forecasting & Solar Irradiance Data, 2023.
[36]. RETScreen, I. (2001). Photovoltaic Project Analysis. Clean Energy Project Analysis, RETScreen Engineering and Cases Text book.
[37]. Kymakis, E., Kalykakis, S., & Papazoglou, T. M. (2009). Performance analysis of a grid connected photovoltaic park on the island of Crete. Energy conversion and management, 50(3), 433-438.
[38]. Kumi, E. N., & Brew-Hammond, A. (2013). Design and analysis of a 1 MW grid-connected solar PV system in Ghana.
[39]. Markvart, T. (Ed.). (2003). Practical handbook of photovoltaics: fundamentals and applications. Elsevier.
[40]. Kalogirou, S. A. (2013). Solar energy engineering: processes and systems. Academic press.
[41]. Marion, B., Adelstein, J., Boyle, K. E., Hayden, H., Hammond, B., Fletcher, T.,& Townsend, T. (2005, January). Performance parameters for grid-connected PV systems. In Conference Record of the Thirty-first IEEE Photovoltaic Specialists Conference, 2005. (pp. 1601-1606). IEEE.
[42]. Short, W., Packey, D. J., & Holt, T. (1995). A manual for the economic evaluation of energy efficiency and renewable energy technologies (No. NREL/TP-462-5173). National Renewable Energy Lab.(NREL), Golden, CO (United States).